Curr Genet (2006) 49: 166–177
DOI 10.1007/s00294-005-0005-6

RESEARCH ARTICLE

**Dilip K. Lakshman · Chunyu Liu · Prashant K. Mishra**
**Stellos Tavantzis**

# Characterization of the *arom* gene in *Rhizoctonia solani*, and transcription patterns under stable and induced hypovirulence conditions

Received: 22 February 2005 / Revised: 19 May 2005 / Accepted: 11 June 2005 / Published online: 15 February 2006


**Abstract** The quinate pathway is induced by quinate in the wild-type virulent *Rhizoctonia solani* isolate Rhs 1AP but is constitutive in the hypovirulent, M2 dsRNA-containing isolate Rhs 1A1. Constitutive expression of the quinate pathway results in downregulation of the shikimate pathway, which includes the pentafunctional *arom* gene in Rhs 1A1. The *arom* gene has 5,323 bp including five introns as opposed to a single intron found in *arom* in ascomycetes. A 199-bp upstream sequence has a GC box, no TATAA box, but two GTATTAGA repeats. The largest arom transcript is 5,108 nucleotides long, excluding the poly(A) tail. It contains an open reading frame of 4,857 bases, coding for a putative 1,618-residue pentafunctional AROM protein. A Kozak sequence (GCGCCATGG) is present between +127 and +135. The 5′-end of the *arom* mRNA includes two nucleotides (UA) that are not found in the genomic sequence, and are probably added post-transcriptionally. Size and sequence heterogeneity were observed at both 5′- and 3′-end of the mRNA. Northern blot and suppression subtractive hybridization analyses showed that presence of a low amount of quinate, inducer of the quinate pathway, resulted in increased levels of *arom* mRNA, consistent with the compensation effect observed in ascomycetes.

Communicated by U. Kück

D. K. Lakshman · C. Liu · P. K. Mishra · S. Tavantzis (✉)
Department of Biological Sciences, University of Maine,
5735 Hitchner Hall, Orono, ME 04469-5735, USA
E-mail: tavantzis@umit.maine.edu
Fax: +1-207-5812801

D. K. Lakshman
USDA-ARS, US National Arboretum,
B-010A, 10300 Baltimore Avenue, Beltsville, MD 20705, USA

C. Liu
B6 Department of Neurology,
Boston University School of Medicine,
715 Albany Street, Boston, MA 02118, USA

P. K. Mishra
Department of Molecular, Cellular and Developmental Biology,
University of California, Santa Barbara, CA 93106, USA

## Introduction

Hypovirulence refers to a condition in which a fungal plant pathogen has a less-than-normal disease-producing capacity. Studies have shown that hypovirulence is caused by nuclear or cytoplasmic genetic factors (Elliston 1982). Fungal double-stranded RNAs (dsRNAs) have been reported to be associated with hypovirulence in fungi (for recent reviews, see Tavantzis 2001).

*Rhizoctonia solani* Kühn (teleomorph, *Thanatephorus cucumeris* (Frank) Donk.), consisting of at least 13 anastomosis groups (AG) (Carling 1996) is a soil-borne plant pathogen attacking numerous plant species (Sneh et al. 1996). Experimental evidence has shown that the M2 dsRNA is associated with hypovirulence (Jian et al. 1997), and is located mainly in the cytoplasm of *R. solani* (Lakshman et al. 1998). All isolates harboring M2 ($M2^+$) are hypovirulent. M2 can be transmitted from $M2^+$ to $M2^-$ (M2-lacking) cultures through hyphal anastomosis, converting $M2^-$ strains from virulent to hypovirulent (Jian et al. 1997).

Plants inoculated with the M2-containing hypovirulent strain of *R. solani*, Rhs 1A1 (AG 3) exhibit a significantly enhanced growth response (Bandy and Tavantzis 1990). In vitro cultures of *R. solani* produce phenylacetic acid (PAA), which is capable of causing the same disease syndrome on potato as the pathogen itself (Boosalis 1950; Sherwood and Lindberg 1962; Wyllie 1962; Frank and Francis 1976). PAA and its metabolites from plant sources are plant growth regulators (auxin) (Chamberlain and Wain 1971; Milborrow et al. 1975). We have shown that the amount of PAA produced by the hypovirulent isolate Rhs 1A1 was only 10% of that produced by virulent AG 3 isolates (Tavantzis et al.

1989; Tavantzis and Lakshman 1995). So, it appears that the amount of PAA produced by virulent AG 3 isolates has phytotoxic (herbicide-like) effects on potato as opposed to the growth-promoting (auxin-like) effects of the low PAA produced by the hypovirulent isolate Rhs 1A1.

M2 codes for polypeptide A (pA) (Liu et al. 2003a), which is phylogenetically related to the suppressor QUTR protein of the quinate pathway and the QUTR-related pentafunctional AROM protein of the shikimate pathway (Lakshman et al. 1998). PAA, a virulence determinant in AG 3 *R. solani*, is a catabolic product of the aromatic amino acid phenylalanine, whose precursor is chorismic acid, the end-product of the shikimate pathway (Fig. 1). The quinate pathway is responsible for the catabolism of quinate to protocatechuate (PCA) in many fungi and bacteria (Fig. 1). Quinate accounts for up to 10% (w/w) of decaying plant matter and can be used as an important carbon source by soil-borne microbes (Davis 1975).

In *Aspergillus nidulans* (Lamb et al. 1996) and *Neurospora crassa* (Giles et al. 1991), QUTR (or its ortholog) binds the transcription activator QUTA (or its ortholog) thus blocking the expression of the quinate pathway. In both of these ascomycetes, environmental quinate brings about induction of the quinate pathway (Giles et al. 1967; Hawkins et al. 1982). Lamb et al. (1992) have shown that dysfunctional QUTR causes a constitutive expression of the quinate pathway genes, thus drawing the shared substrates, DHQ and DHS (Fig. 1), away from the shikimate pathway, and, in turn, drastically reducing aromatic amino acid (and PAA) synthesis. The M2-encoded pA lacks the domain of QUTR that blocks the transcription activation domain (TAD) of QUTA (Lakshman et al. 1998). So, we hypothesized that binding of pA (a putative truncated repressor) to the *R. solani* QUTA ortholog may allow the TAD of QUTA to interact with the transcription preinitiation complex and thus allow the constitutive transcription of the quinate pathway (Lakshman et al. 1998).

We have recently reported data supporting the above hypothesis: (1) polypeptide pA and its corresponding mRNA are detectable in hypovirulent ($M2^+$) *R. solani* cultures but not in virulent cultures lacking M2 ($M2^-$) cultures; (2) the quinate pathway is constitutively expressed whereas the shikimate pathway (*arom* gene) is downregulated in $M2^+$ cultures and, (3) the relative concentration of phenylalanine, a precursor of PAA, is directly proportional to virulence in $M2^-$ but not in $M2^+$ cultures (Liu et al. 2003a). We have also shown that in the virulent isolate Rhs 1AP, quinate brings about a dramatic reduction of virulence and induces synthesis of the M2-encoded polypeptide pA and its respective mRNA. The quinic-acid-induced hypovirulence in Rhs 1AP could not be overturned by chorismic acid, which otherwise enhances the virulence of Rhs 1AP dramatically (Liu et al. 2003b).

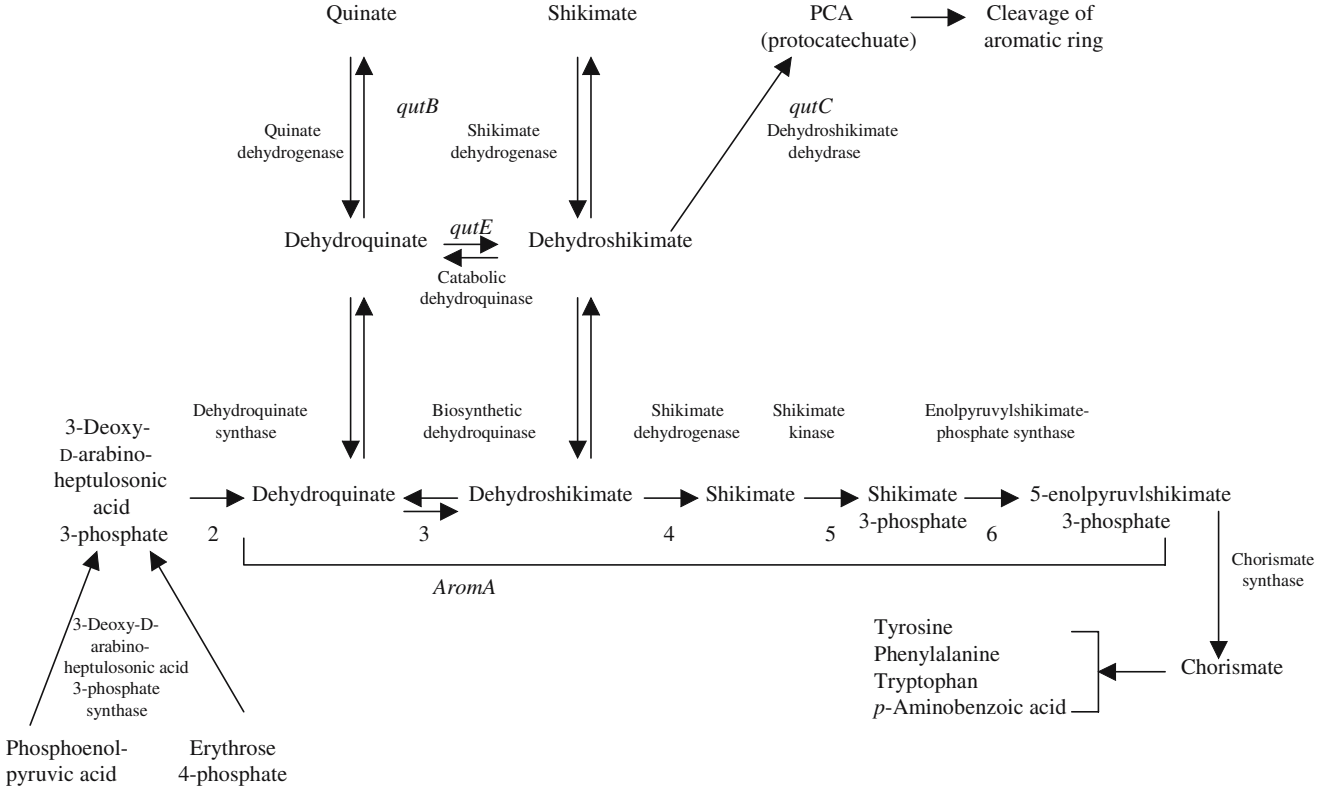


**Fig. 1** The genes, enzymes, and metabolites comprising the quinate and shikimate pathways in *Aspergillus nidulans* (from Lamb et al. 1992)

The purpose of this study was to characterize the *arom* gene in *R. solani*. In yeast, filamentous fungi and some protists, steps 2 to 6 of the shikimate pathway are catalyzed by a pentafunctional enzyme, the AROM protein (Fig. 1), which is encoded by a single gene, the *arom* gene (Charles et al. 1986; Hawkins et al. 1993). Unveiling of the expression patterns of this gene might help us understand the molecular basis of virulence regulation in *R. solani*. This is the first report on characterization of the *arom* gene in a basidiomycete. The deduced *R. solani* AROM polypeptide possesses all of the highly conserved motifs and enzyme domains found in AROM proteins from ascomycetes but has five introns as opposed to the single intron present in its homolog from ascomycetes. Data presented in this report indicate that in wild-type *R. solani*, transcription of the *arom* mRNA is increased upon induction of the quinate pathway. Finally, we discuss these results in relation to previous reports on relative expression levels of the *arom* gene in ascomycetes, when the quinate pathway is switched on in the absence of environmental quinate.

## Materials and methods

### Fungal cultures and media

Vogel's minimal salts solution (Davis and deSerres, 1970) containing 20 mM glucose is referred to as liquid 'glucose minimal media.' Similarly, Vogel's minimal salts solution containing either quinate (26 mM) or glycerol (20 mM) as a sole carbon source is referred to as liquid 'quinate minimal media' or liquid 'glycerol minimal media' (Lamb et al. 1992). Quinate-induced or control mycelial cultures of *R. solani* isolates Rhs 1AP and Rhs 1A1 were prepared as described previously (Liu et al. 2003a and 2003b).

### Complementary DNA (cDNA) cloning of the *arom* mRNA

Total RNA was extracted from the Rhs 1AP isolate of *R. solani* using the method of Logemann et al. (1987). The strategy for cDNA cloning is illustrated in *Panel A* of Fig. 2. Degenerate primers (EPSP1 and EPSP2) were derived from consensus sequences of three AROM polypeptides (*Saccharomyces cerecisiae*, *Aspergillus nidulans*, and *Pneumocystis carinii*). EPSP1 was derived from the consensus sequence GNAGTA (residues 586–591 of the *A. nidulans* AROM protein), and EPSP2 from the consensus sequence KECNRI (residues 752–758 of the *A. nidulans* AROM protein) of the EPSP domains (Table 1). RT-PCR was carried out using total RNA from *R. solani* and the above degenerate primers. A PCR product of 850 bp was cloned and sequenced. Blast N and Blast X searches in the GENBANK confirmed that this was a partial *arom* clone. Using other upstream and downstream conserved primers as well as end-specific primers from the above clone, the rest of the *arom* mRNA was cloned and sequenced. One pair of primers included degenerate primer DHQ3 (Table 1) from the consensus sequence GGGVIGD (residues 113–118 of the *A. nidulans* AROM protein) of the DHS domain and an end-specific primer EPSP3 (downstream, Table 1). Another pair included an end-specific primer EPSP4 (upstream, Table 1) and an anchor primer 5′-AAGCTTTTTTTTTTTTTTA-3′. A 5′-RACE (rapid amplication of cDNA ends) reaction was employed using SuperScript II RT polymerase (Gibco BRL) for reverse transcription in a two-step RT-PCR to clone the 5′-end of *arom* cDNA.

### Cloning of the *arom* genomic DNA sequence

PCR of genomic DNA from Rhs 1AP was carried out using selected primers from the *R. solani arom* cDNA sequence. Genomic DNA was partially digested with endonuclease *Eco*RI since no such restriction sites were detected in the *R. solani arom* cDNA sequence to minimize shearing of DNA and improve the effciency of PCR. *Arom*-specific PCR products were separated and eluted from agarose gels using the QIA quick PCR Purification Kit (QIAquick, Quagen Inc., Mississauga, ON, Canada) and sequenced. The strategy for cloning the *arom* genomic DNA is depicted in *Panel B* of Fig. 2. All of the primers used in genomic DNA cloning are listed in Table 1.

The sequence upstream from the transcription initiation site of *arom* gene was cloned using the Single Specific Primer-Polymerase Chain Reaction (SSP-PCR) technique (Sambrook et al. 1989 Shyamala and Ferro-Luzzi Ames, 1993). Genomic DNA of Rhs 1AP was digested with the restriction endonuclease *Sac*I (New England Biolabs Inc., Beverly, MA, USA). Plasmid pBluescript II SK(-) (Stratagene, La Jolla, CA, USA) was also digested with both *Xho*I and *Sac*I enzymes. The double-digested plasmid and the *Sac*I-digested genomic DNA were ligated at the *Sac*I site. PCR reactions were carried out using a primer (PBSK2) (Table 1) from the plasmid and a primer (AROMP1) (Table 1) near the 5′-end of the *arom* gene. Nested PCR was carried out with the vector-specific nested primer (PBSK1) (Table 1) and a gene-specific nested primer (AROMP2) (Table 1). The nested PCR product was cloned in Topo XL cloning vector (Invitrogen Corporation, Carlsbad, CA, USA) and sequenced with a vector-specific primer. This procedure allowed determination of an additional sequence of 199 bp located upstream of the *R. solani arom* gene.

### Sequence and phylogenetics analyses

Genomic or cDNA sequences were determined by the Sanger dideoxy method using cycle sequencing with an ABI 3730 DNA Analyzer, and the ABI Prism DNA

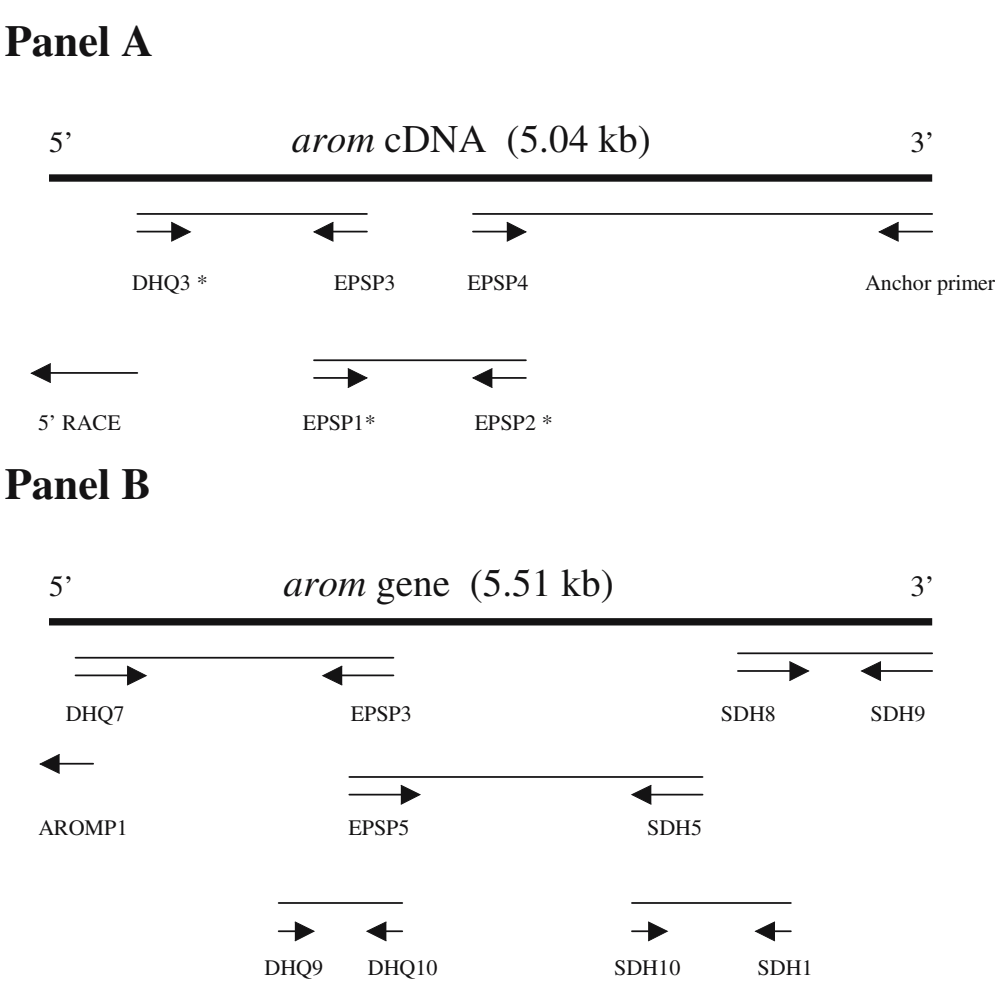


**Fig. 2** Schematic overview of the strategy used in cDNA cloning (*Panel A*) and amplification from genomic DNA (*Panel B*) of the *arom* gene of *R. solani*. *Panel A*: Degenerate primers (*asterisk*) were selected from the consensus sequences of three AROM polypeptides (*Saccharomyces cerecisiae*, *Aspergillus nidulans*, and *Pneumocystis carinii)*. The initial PCR product was obtained by RT-PCR using two degenerate primers, EPSP1 and EPSP2 (see text). This sequence was extended to the 5′-end by RT-PCR using degenerate primer DHQ3 and the end-specific primer EPSP3 (selected from the initial cDNA clone). 5′-RACE reactions were carried out to clone the 5′-end of the *arom* mRNA. The initial sequence was extended to the 3′-end by RT-PCR using the end-specific primer EPSP4 (selected from the initial cDNA clone) and an anchor primer. Total RNA from the *R. solani*. isolate Rhs IAP was used as a template in the RT-PCR reactions. *Panel B*: The overlapped lines denote PCR reactions using the end-specific primers selected from the *R. solani* cDNA clone. The upstream promoter region was cloned by a specifically designed PCR reaction (see text for details). Primer sequences used in the above PCR reactions are listed in Table 1

sequencing software version 5.0 as described previously (Strauss et al. 2000).

The AROM protein sequences from 16 ascomycete and 2 basidiomycete fungal species were obtained from the GenBank database (see legend of Fig. 4) and were compared with the AROM sequences of *R. solani* (teleomorph, *Thanatephorus cucumeris*) generated in our study. The AROM sequence of *Toxoplasma gondii* (Campbell et al. 2004) was included in the alignment for outgroup comparisons. The protein sequences were edited manually after an initial alignment using the BLOSUM62 sequence alignment algorithm as installed in the software BioEdit (Hall 1999). Phylogenetic analysis was performed using the software MEGA2 (Kumar et al. 2001) with the JTT model of amino acid evolution, which corrects for multiple amino acid substitutions. A phylogenetic tree was produced by neighbor-joining clustering procedure (Saitou and Nei 1987) and stability of clades was assessed by 1000 bootstrap replicates.

## Expression of the *arom* gene in quinate-induced or uninduced $M2^+$ and $M2^-$ isolates

### *Northern blot hybridization analysis*

Total RNA was extracted from mycelial cultures of the virulent $M2^-$ isolate Rhs 1AP and the hypovirulent $M2^+$ Rhs 1A1 isolate grown in the presence or absence of quinate as described above. The amounts of total RNA were calibrated by agarose gel electrophoresis, followed by a northern blot hybridization analysis using

**Table 1** Nucleotide sequences of primers used for PCR-mediated amplification of the *arom* gene cDNA and genomic DNA of the *R. solani* culture Rhs 1AP

| Primer | Nucleotide sequence (5′ to 3′) |
|---|---|
| EPSP1 | GGNAAYGCNGGNACNGC |
| EPSP2 | DATNCKRTTRCAYTCYTT |
| DHQ3 | ACHGGNGGNGGNGTNATHGG |
| EPSP3 | AGACAGTGGTGAGGAAGCGA |
| EPSP4 | GTATTGCCAACCAACGTGTC |
| DHQ7 | CGATTCCAACGACAGCGCAC |
| DHQ9 | CAAGAGCATCTCCAACCGTG |
| DHQ10 | TGAGACCGCCAGCACCAATG |
| EPSP5 | TCGCTTCCTCACCACTGTCT |
| SDH1 | GTACCAAACAGACTCGTGGA |
| SDH5 | GCCACGATGCGATGATCTGA |
| SDH8 | CTCAGATCATCGCATCGTGG |
| SDH9 | GCGCCGAAACGCTGATCTTG |
| SDH10 | TTGCGCCACACCTCGTCTCT |
| AROMP1 | CGCGTGTCGGTAATAAGAAC |
| AROMP2 | GATTAGTGAGGACTGTATCG |
| PBSK1 | TGACCATGATTACGCCAAGC |
| PBSK2 | CTTCCGGCTCGTATGTTGTG |

a $\beta$-tubulin cDNA, radioactively-labeled probe. Signal intensities of the $\beta$-tubulin bands were measured with a LKB Model Ultroscan XL Enhanced Laser Densitometer (Pharmacia LKB Biotechnology, Upsala, Sweden) using Gelscan XL software. The amounts of total RNA were adjusted on the basis of the signal intensities of the respective $\beta$-tubulin bands, and a second northern blot hybridization analysis was conducted using an *arom* cDNA radiolabeled probe. The intensities of the arom-hybridizing bands were estimated using the NIH Image software (http://rsb.info.nih.gov/nih-image/Default.html). The $\beta$-tubulin gene sequence of *R. solani* (AG 3) was provided by Dolores González (Laboratorio de Sistemática Molecular Instituto de Ecología, A. C., Mexico).

### *Suppression subtractive hybridization analysis*

Suppression Subtractive Hybridization (SSH) (Diatchenko et al. 1996) was used to compare *arom* mRNA populations in quinate-induced Rhs 1AP and untreated Rhs 1AP, and thus determine whether the results of the northern blot analysis could be confirmed. Total RNA was extracted using TRIZOL (Invitrogen life technologies, Carlsbad, CA 92008, USA) as described by the manufacturer, and poly(A) RNA was obtained using the PolyATract mRNA Isolation System IV kit (Promega, Madison, WI, USA). For SSH, we used the Clontech PCR-Select cDNA Subtraction Kit (BD Biosciences Clontech, Palo Alto, CA 94303, USA). Normalization of cDNA was checked using the BD Advantage 2 PCR enzyme kit (BD Biosciences Clontech) and primers specific for the *R. solani* (AG 3) glyceraldehyde-3-phosphate dehydrogenase (GP3DH) (GeneBank Accession No. AF339929) or the *R. solani*-(AG 3)-specific $\beta$-tubulin gene sequence. The *R. solani* AG-3-specific G3PDH 3′ primer was RsG3PDH 4 (5′-TTCTTGAGG GCAGCTTTGAT-3′) and the G3PDH 5′ primer was RsG3PDH 3 (5′-ACTCAAAAGACGGTTGACGG-3′). The expected size of the G3PDH PCR product was 242 bp. Subtraction efficiency of a second housekeeping gene, $\beta$-tubulin gene of *R. solani* (AG 3), was verified using the tubulin3 (5′-GCACCCTCAAGCTCTCCA-3′) and tubulin4 (5′-AGTTGAGCTGACCAGGGAAA-3′) primers (based on the sequence provided by Dolores González (Laboratorio de Sistemática Molecular Instituto de Ecología, A. C., Mexico). The expected size of the $\beta$-tubulin PCR product was 105 bp.

Prior to determining the level of transcription of the *arom* gene mRNA in the relevant cultures, we conducted standardization of the $\beta$-tubulin gene in quinate-induced and uninduced Rhs 1AP. A dilution series of total cDNA [obtained from poly(A) RNA samples] were subject to PCR using the $\beta$-tubulin-specific primers tubulin3 and tubulin4, and the amounts of the respective PCR products were assessed at different numbers of cycles. To compare *arom* mRNA levels in the respective cultures, we selected dilutions of quinate-induced and uninduced cDNA that gave the same PCR product band intensities at different PCR cycle numbers using the $\beta$-tubulin primers. The primers used for this comparison were Arom1a (5′-GAAAAAGCGAGCGACAGTG-3′) and Arom1b (5′-CACCCAGCCAGAAGACTTG-3′), and the amounts of the expected PCR product were assessed at different times (number of cycles) during amplification. The expected size of the *arom* PCR product was 152 bp.

## Results

### Sequence analysis of the *arom* gene from *R. solani*

The *R. solani arom* gene consists of 5,323 bp (GeneBank accession number AF 482690.1). This total includes a 5′-end UTR (131 bp), the ORF (4,857 bp), total introns (243 bp), and a 3′ UTR (92 bp). A 199-bp upstream partial promoter sequence is shown in Fig. 3 (*Panel A*). The *arom* gene possesses five introns (530–580, 789–836, 1,623–1,670, 2,671–2,718, and 2,940–2,987 bases in reference to the start site of the largest transcript and in GeneBank accession number AF 482690.1). The first intron consists of 51 bp, the rest are 48 bp each. All of the introns start with GT and end with AG.

Based on analyses of 10 RACE clones from the 5′-end and 12 cDNA clones from the 3′-end, we observed transcript heterogeneities at both ends. Variations at the 5′-end of RACE clones existed both in terms of size (data not shown) and sequence (Fig. 3, *Panel A*). A description of the 5′-end variability is given in the legend of Fig. 3. Based on RACE analysis at least five size variations and several base substitutions were observed at the 5′-end. The largest transcript is 15 nucleotides longer than the smallest transcript at the 5′-end. In contrast, we could only detect two size variations and no

## Panel A

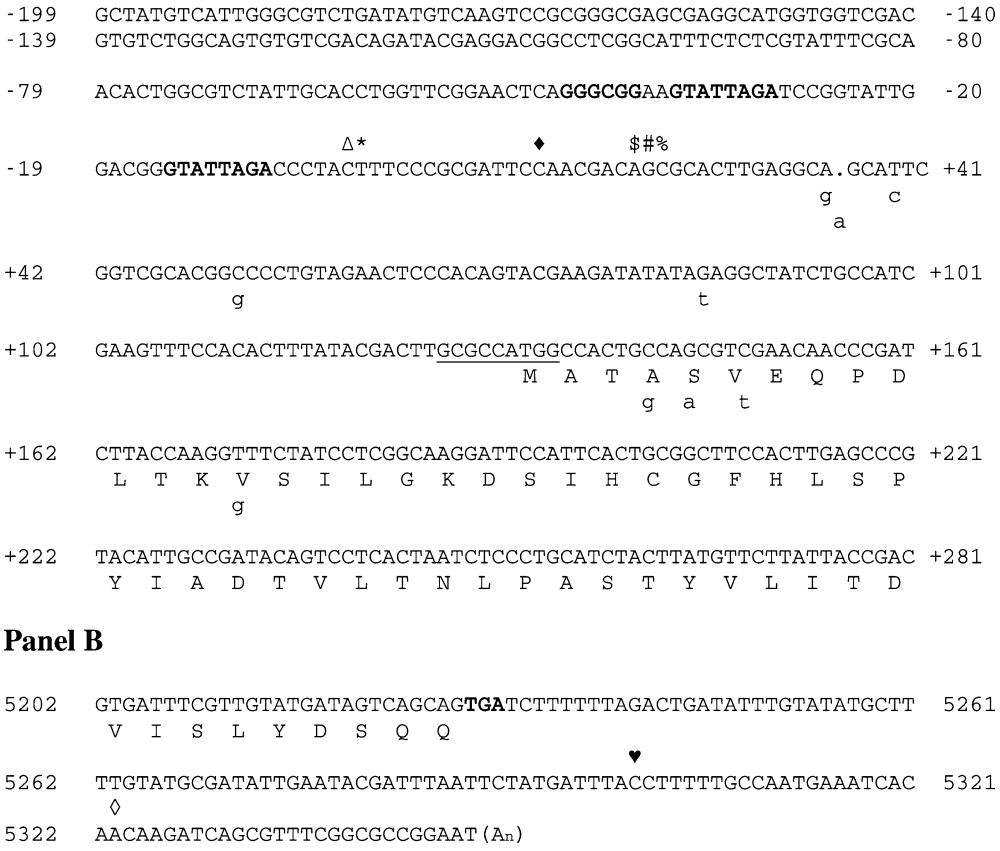


## Panel B




**Fig. 3** Genomic nucleotide and amino acid sequences at the 5′-terminus (*Panel A*) or the 3′-terminus (*Panel B*) of the *R. solani arom* gene. *Panel A*: Nucleotides are numbered relative to the start of the sequence of the longest transcript, denoted by an *asterisk* at the top of the nucleotide. The starting nucleotide of the shortest transcript detected has been denoted with a *filled diamond* sign at the top of the nucleotide. Some other transcript start sites derived from 5′-RACE clones are denoted by $, #, and % signs. The GC box sequences and the octanucleotide (GTATTAGA) repeats at a 15-nucleotide interval are shown in *bold letters*. Kozak consensus sequence (GCGCCATGG) (Kozak 1987) is *underlined*. A gap was introduced in the genomic sequence following nucleotide number +35 to allow positioning of an adenine nucleotide insertion in one of the 5′-RACE clones. The 199-nucleotide upstream sequence (*numbered in negative*) is not present in the GenBank accession AF 482690.1. Two nucleotides (AT) present at the extreme 5′-end of the largest RACE sequence are not present in the genomic sequence at the point denoted by a Δ sign. Nucleotides in *lower case letters* denote base substitutions observed in individual RACE clones. Amino acid sequences start with methionine (M), and are shown in *upper case letters* beneath the nucleotide sequence. *Panel B*: The stop codon is indicated in *bold letters*. The small transcript of the *arom* gene starts polyadenylation at the site denoted by the *filled heart* symbol. The end of the genomic sequence reported in GenBank accession AF 482690.1 has been marked by the *open diamond* symbol. Nucleotides are numbered as in the GenBank accession AF 482690.1 in both panels

mutations in the 3′-end clones (Fig. 3, *Panel B*). Excluding the poly(A) tail, the largest mRNA was 49 nucleotides longer than the smallest transcript at the 3′-end (Fig. 3, *Panel B*). We have not determined the exact length of poly-A tails from the two 3′-end size variants. The largest *arom* cDNA, assembled from PCR and 5′ RACE experiments, has 5,108 nucleotides. It is comprised of a 133-nucleotide 5′-end UTR, containing the 2-nucleotide (UA) addition, a 4,857-nucleotide ORF, and a 118-nucleotide 3′-end UTR, excluding the poly(A) tail. The first two nucleotides (UA) at the 5′-end of the mRNA were not represented in the corresponding genomic sequence and they were presumed to have been added post-transcriptionally.

The promoter region had a GC box (GGGCGG) sequence (−45 to −40) and a Kozak sequence GCGCCATGG (+127 to +135) (Kozak 1987), but lacked a TATAA box sequence. Interestingly, two repeats, GTATTAGA, which were 15 bp apart, were found just upstream of the transcription initiation site.

## Phylogenetic analysis

Three blocks of the multiple sequence alignment of the AROM proteins from 16 ascomycetes and 3 basidiomycetes are shown in Fig. 4. The *R. solani* (designated as T. cuc) AROM protein contains the highly conserved

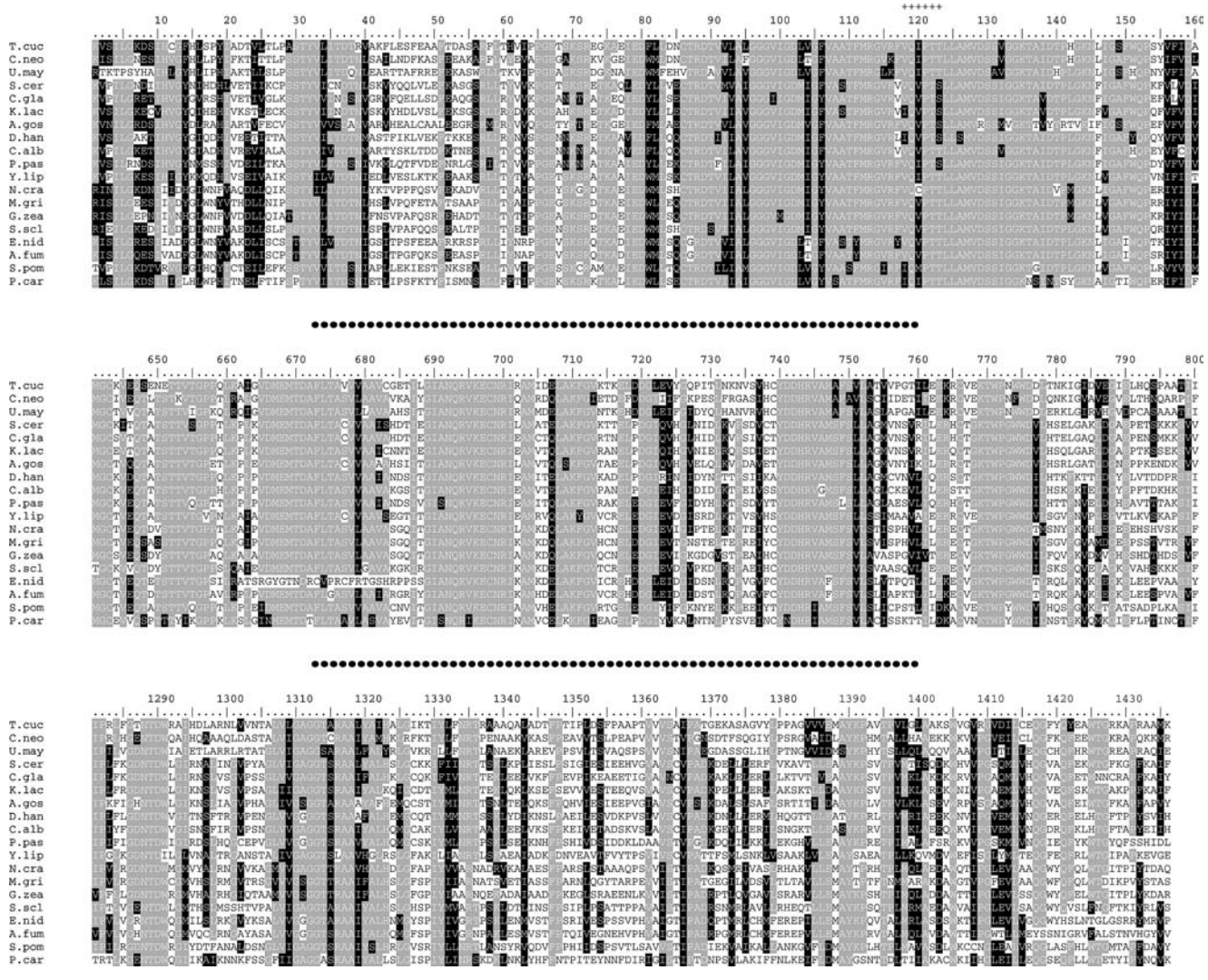


**Fig. 4** Comparison of the amino acid sequence of the AROM polypeptide from *R. solani* (*T. cucumeris*) with those of the 2 other basidiomycetes and 16 ascomycetes. Three representative regions (amino- and carboxyl-terminals and a middle portion) are shown here. *Gray boxes* indicate identical residues, and *black boxes* indicate similar residues. The numbering in this figure is based on the alignment scheme of the software and does not correspond to amino acid number of any of the AROM proteins. The dinucleotide binding motif GXGXXG (118–123 aa) of *Thanatephorus cucumeris* (*R. solani*) AROM DHS domain is indicated by + signs. The purine nucleotide binding motif G/AXXXXGKT/S (901–908 aa) of SK domain, the LGNAGTA motif (497–503 aa) of EPSP domain, and the DHR signature motif (832–834 aa) of EPSP are located in highly conserved regions of the AROM protein (not shown here). AROM amino acid sequences were obtained from the following sources: T. cuc (*T. cucumeris*; GenBank Accession No. AF482690; Liu et al. 2003a), C. neo (*Cryptococcus neoformans*; GenPept Accession No. AAW41820.1), U. may (*Ustilago maydis*; GenPept Accession No. EAK84510.1) S. cer (*Saccharomyces cerevisiae*; GenBank Accession No. NP010412.1; Duncan et al. 1987), C. gla (*Candida glabrata*; GenBank Accession No. XM449840; Dujon et al. 2004), K. lac (*Kluveromyces lactis*; Accession No. XM455965; Dujon et al. 2004), A. gos (*Ashbya gossypii*; GenPept Accession No. AAS54555.1), D. han (*Debaryomyces hansenii*; GenBank Accession No. XM459982; Dujon et al. 2004), C. alb (*Candida albicans*; GenPept Accession No. EAL04039.1), P. pas (*Pichia pastoris*; GenPept Accession No. AAW33954.1), Y. lip (*Yarrowia lipolytica*; RefSeq Accession No. XM_505337; Dujon et al. 2004), N. cra (*Neurospora crassa*; GenPept Accession No. CAD21207.1; Coggins et al. 1987a and b), M. gri (*Magnaporthe grisea*; GenPept Accession No. EAA49470.1), G. zea (*Gibberella zeae*; GenPept Accession No. EAA73613.1), S. scl (*Sclerotinia sclerotiorum*; GenBank Accession No. AY746008; Yu et al. 2004), E. nid (*Emericella nidulans* Swiss-Prot Accession No. P07547; Charles et al. 1985), A. fum (*Aspergillus fumigatus;* GenPept Accession No. CAD29607; Pain et al. 2004), S. pom (*Schizosaccharomyces pombe*; GenBank Accession No. NP594681; Wood et al. 2002), P. car (*Pneumocystis carinii*; Swiss-Prot Accession No. Q12659; Banerji et al. 1993), T.gon (*Toxoplasma gondii*; GenPept Accession No. AAQ83833.1; Campbell et al. 2004)

motifs and the five domains of the respective enzymes found in characterized AROM polypeptides [*A. nidulans*, *N. crassa*, *S. serevisiae* (Duncan et al. 1987)] or deduced AROM polypeptides from other ascomycetes and basidiomycetes (Fig. 4). The *R. solani* AROM protein showed a significant amino acid sequence similarity with the other fungal AROM proteins. The sequence identity between the *R. solani* AROM protein

and those of the other two basidiomycetes ranged between 59.9% and 62.7%. The identity range between the *R. solani* AROM protein was 52–54.5% with AROM proteins from filamentous ascomycetes, and 48–54% with those from yeasts and archiascomycetes. In contrast, the AROM protein from the protist *Toxoplasma gondii* had a low degree of identity (26.4–29.9%) with the fungal AROM proteins.

The phylogenetic tree of Fig. 5 shows the relationships between the AROM proteins from 16 ascomycetes and 3 basidiomycetes including *R. solani* (teleomorph *T. cucumeris*). A neighbor-joining tree drawn using a bootstrap resampling procedure demonstrated a clear distinction between AROM proteins of ascomycetes and basidiomycetes (Fig. 5). Sixteen ascomycetes were separated into three well-resolved groups: Eight genera were members of *Saccharomycetales* (Group A, with 99% bootstrap support); six genera of filamentous ascomycetes were grouped together (Group B with a 100% bootstrap support) and; two genera from Archiascomycetes were resolved in Group C. Three basidiomycetes formed a monophyletic group with a 100% bootstrap support that was well-resolved from the ascomycetous groups. The AROM of *Toxoplasma gondii* (Protista) was used as the root taxon.

## Transcription levels of the arom mRNA

Northern blot hybridization analysis was conducted with quinate-induced (6 h) or uninduced total RNA extracts from hypovirulent Rhs 1A1 and virulent Rhs 1AP. A long (18 h) quinate induction was included for Rhs 1A1, in which the quinate pathway is constitutive (Liu et al. 2003a). The data showed that in both isolates, the amount of *arom* mRNA was greater in quinate-induced extracts than in their uninduced counterparts (Fig. 6b). Moreover, long quinate induction in Rhs 1A1 resulted in an increased level of *arom* mRNA as compared to that of short induction.

For suppression subtractive hybridization analysis, cDNA from quinate-induced Rhs 1AP was subtracted with excess cDNA from untreated Rhs 1AP, and was checked for normalization of two constitutive genes, G3PDH (Fig. 7, *left panel*), and $\beta$-tubulin (Fig. 7, *right panel*). In the case of the G3PDH gene, the respective PCR product became slightly visible after 31 cycles of amplification of subtracted cDNA, whereas an abundant amount of PCR product was generated after 19 cycles of amplification of unsubtracted cDNA. Similarly, the $\beta$-tubulin gene PCR product became visible following 33 cycles of amplification of subtracted cDNA, but after only 18 cycles of amplification of unsubtracted cDNA. So, results regarding these constitutive genes indicated that subtraction was efficient and as expected, that is, in the subtracted sample, the PCR product should be observed about 5–15 cycles later than in the unsubtracted.

We then carried out PCR amplification of $\beta$-tubulin using a series of dilutions of quinate-induced and uninduced Rhs 1AP cDNA. The respective dilutions (of the two cDNA preparations) that resulted in almost identical amounts of the expected PCR product were further compared at various PCR cycles. The DNA band intensities of the $\beta$-tubulin PCR product in the two cDNA samples were the same for all the step cycles tested (Fig. 7b). Subsequently, an *arom*-specific PCR was carried out with the two standardized cDNA dilu-

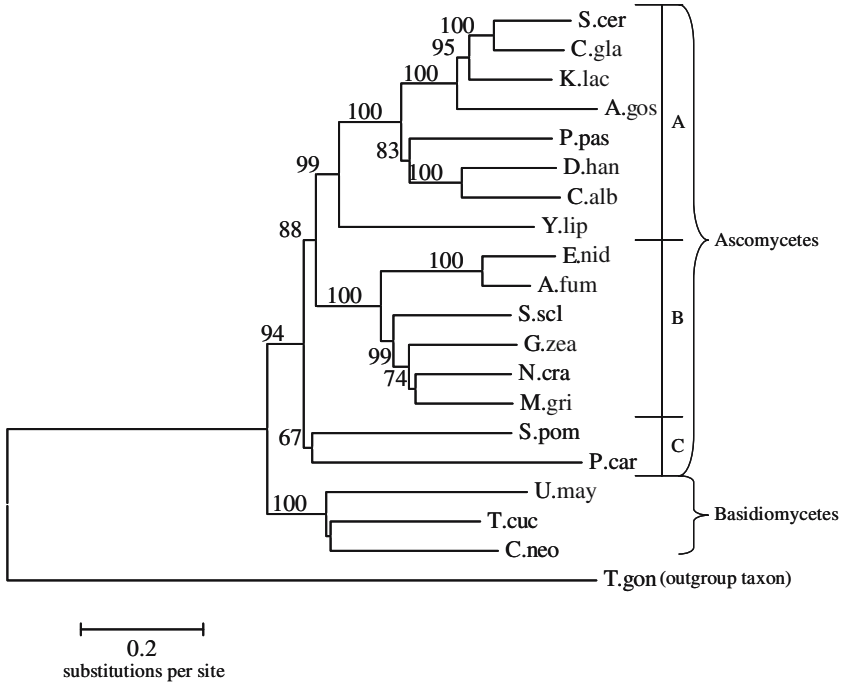


**Fig. 5** The neighbor-joining phylogram showing phylogenetic relationships among 19 fungal AROM protein sequences. The phylogeny was drawn using JTT model of amino acid evolution as installed in the software MEGA2 (Kumar et al. 2001) and was rooted with AROM protein of the protist *Toxoplasma gondii*. *Bar* represents amino acid substitutions per site, and *numbers above branches* represent bootstrap support values. AROM sequences and the accession numbers are given in the legend of Fig. 4

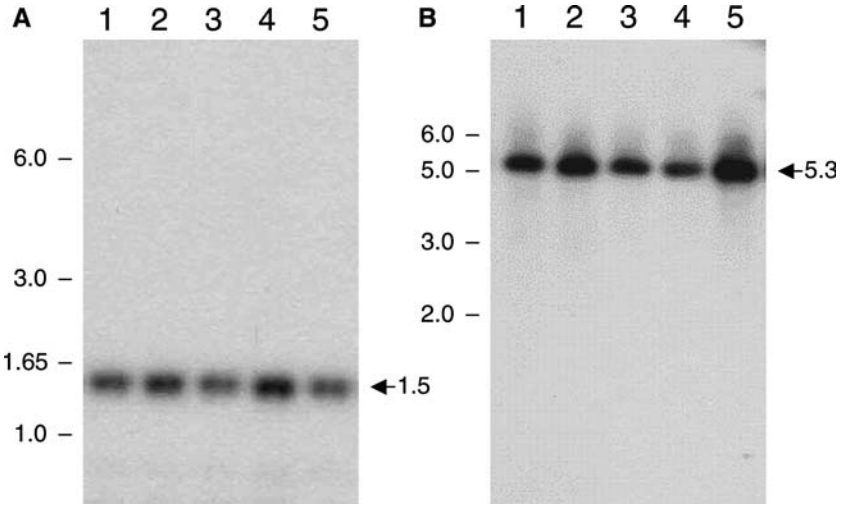


**Fig. 6** Comparison of the relative amounts of the *arom* gene transcript in the $M2^-$ virulent Rhs 1AP and the $M2^+$ hypovirulent Rhs 1A1 by Northern blot hybridization analysis. **a** Total RNA samples from quinate-induced Rhs 1A1 (5 h post-induction) (*lane 1*), quinate-induced Rhs 1A1 (18 h post-induction) (*lane 2*), untreated Rhs 1A1 (*lane 3*), untreated Rhs 1AP (*lane 4*) and quinate-induced Rhs 1AP (18 h post-induction) (*lane 5*) were hybridized with a radiolabeled *β*-tubulin-specific probe. **b** The amounts of total RNA from the samples shown in (**a**) were adjusted on the basis of the *β*-tubulin-hybridizing band intensities (see text), and the adjusted amounts were loaded on a second gel in the same order as above. An *arom* cDNA-specific, $^{32}$P-labeled probe, generated using primers EPSP1 and EPSP2 (Table 1), was used to determine the relative amounts of *arom* mRNA occurring in quinate-induced Rhs 1A1 (5 h post-induction; 11,642 pixels) (*lane 1*), quinate-induced Rhs 1A1 (18 h post-induction; 15,869 pixels) (*lane 2*), untreated Rhs 1A1 (10,630 pixels) (*lane 3*), untreated Rhs 1AP (9,162 pixels) (*lane 4*) and quinate-induced Rhs 1AP (18 h post-induction; 24,186 pixels) (*lane 5*) The intensities of the *arom*-hybridizing bands (expressed in pixels) were measured using the NIH Image software. *Numbers on the left* of each panel show the sizes (in Kb); *bars* indicate the positions of DNA size standards. *Numbers on the right* show the sizes; *arrows* indicate the positions of the *β*-tubulin (**a**) and *arom* (**b**) transcripts

tions. As can be seen in Fig. 7c, the *arom*-specific PCR product became detectable at an earlier amplification cycle in quinate-induced cDNA than the uninduced cDNA. Moreover, the PCR product band intensities generated from quinate-induced cDNA were greater than those from uninduced cDNA at the corresponding step cycles.

## Discussion

This is the first report documenting the characterization of an *arom* gene from a basidiomycete, *R. solani*. The *R. solani arom* gene contains five introns that are located in the 5′-end proximal one-half of the gene as compared to the absence of introns in the *S. cerevisiae arom* gene (Duncan et al. 1987). In contrast, the *A. nidulans arom* gene had been reported to be a 4,812 bp open reading frame (Charles et al. 1986). A more recent work showed that a 53 bp intron is present in the extreme C-terminus of the shikimate dehydrogenase domain (Lamb et al. 1996). Similarly, one intron has been identified in the middle of the dehydroquinate synthase domain of the *P. carinii arom* gene (Banerji et al. 1993).

Several reports show that a single gene can yield mRNA transcripts varying at both 5′- and in 3′-ends. Possible mechanisms for such heterogeneity may involve more than one promoter, alternative splicing leading to inclusion or deletion of exons and introns or the presence of multiple polyadenylation and/or transcription initiation or termination signals (Hickok et al. 1986; Pauws et al. 2001; Jianqiang et al. 2003). Although the exact locations and identities of promoter elements have not been determined experimentally in this study, a repeat of GTATTAGA upstream of the Kozak sequence (GCGCCATGG) at a 15-nucleotide interval, in conjunction with the fact that the largest mRNA was 15 nucleotides longer than the smallest one at the 5′-end (Fig. 3, *Panel A*), may suggest involvement of a bifunctional promoter in *R. solani arom* gene transcription. Moreover, in the absence of a canonical polyadenylation signal (AAUAAA) from the 3′-ends of the two mRNA species, it is difficult to explain size heterogeneity at the 3′-end. The thymidine-rich sequences at the 3′-end UTR may be involved in transcript processing. Analyses of the 3′-end formation of *Saccharomyces cereviseae* transcripts revealed no highly conserved sequence motifs equivalent to AAUAAA (Guo and Sherman 1996).

A search of the predicted AROM protein of *R. solani* in the NCBI Conserved Domain database (v2.02) (Marchler-Bauer and Bryant 2004) and in the pfam database (Sanger Institute, UK) revealed identity with all five domains (DHQ synthase, EPSP synthase, shikimate kinase, dehydroquinase I, and shikimate dehydrogenase), arranged in the same order as established in fungi (Duncan et al. 1987; Banerji et al. 1993). A dinucleotide binding motif (GXGXXG) (Rossman et al. 1974) and a purine nucleotide-binding type A motif (G/AXXXXGKT/S) (Walker et al. 1982) were found in the

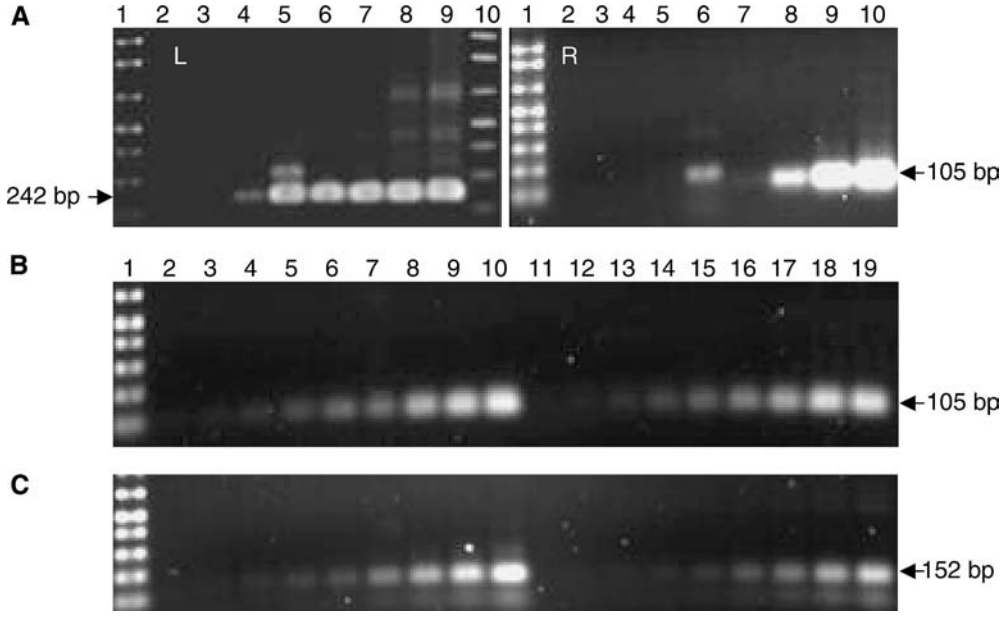


**Fig. 7** Assessment of relative amounts of *arom* mRNA in quinate-induced Rhs 1AP and uninduced Rhs 1AP. **a** Normalization of abundance of cDNA corresponding to glyceraldehyde-3-phosphate dehydrogenase (G3PDH) (*L*) and *β*-tubulin (*R*), respectively, in quinate-induced Rhs 1AP cDNA (tester) subtracted by cDNA from uninduced Rhs 1AP (driver). *Left panel*: *lanes 1* & *10*: DNA size standards, 1 Kb Plus DNA ladder; *lanes 2, 3, 4* & *5*: G3PDH-specific PCR product of subtracted quinate-induced Rhs 1AP cDNA (tester); *lanes 6, 7, 8* & *9*: PCR of uninduced and unsubtracted Rhs 1AP cDNA (driver); *lanes 2* & *6*: 19 cycles; *lanes 3* & *7*: 25 cycles; *lanes 4* & *8*: 31 cycles; *lanes 5* & *9*: 37 cycles. *Right panel*: *lane 1*: DNA size standards, 1 Kb Plus DNA ladder; *lanes 2, 3, 4* & *5*: *β*-tubulin-specific PCR product of quinate-induced Rhs 1AP subtracted cDNA (tester); *lanes 6, 7, 8* & *9*: PCR of uninduced and unsubtracted Rhs 1AP cDNA; *lanes 2* & *6*: 18 cycles; *lanes 3* & *7*: 23 cycles; *lanes* & *8*: 28 cycles; *lanes 5* & *9*: 33 cycles. **b** Calibration of relative concentrations demonstrating equivalence of *β*-tubulin-specific PCR products obtained from cDNA samples of quinate-induced Rhs 1AP (*lanes 2–10*) and uninduced Rhs 1AP (*lanes 11–19*) at different numbers of PCR cycles; *lanes 2* & *11*: 18 cycles; *lanes 3* & *12*: 19 cycles; *lanes 4* & *13*: 20 cycles; *lanes 5* & *14*: 21 cycles; *lanes 6* & *15*: 22 cycles; *lanes 7* & *16*: 23 cycles; *lanes 8* & *17*: 24 cycles; *lanes 9* & *18*: 25 cycles; *lanes 10* & *19*: 26 cycles. DNA size standards (1 Kb Plus DNA ladder) were loaded on *lane 1* of the 1.5% agarose gel. **c** Comparison of relative amounts of *arom* gene-specific mRNA in quinate-induced Rhs 1AP (*lanes 2–10*) and uninduced Rhs 1AP (*lanes 11–19*). Dilutions of cDNA, obtained from quinate-induced and uninduced cDNA, which gave uniform intensity of PCR product at different PCR cycle numbers with *β*-tubulin-specific primers (**b**), were selected for comparison; *lane 1*: DNA size standards (1 Kb Plus DNA ladder); *lanes 2* & *11*: 25 cycles; *lanes 3* & *12*: 26 cycles; *lanes 4* & *13*: 27 cycles; *lanes 5* & *14*: 28 cycles; *lanes 6* & *15*: 29 cycles; *lanes 7* & *16*: 30 cycles; *lanes 8* & *17*: 31 cycles; *lanes 9* & *18*: 32 cycles; *lanes 10* & *19*: 33 cycles. *Arrows* (on the right or left of each panel) show the positions, and *numbers* indicate the sizes (in bp) of the PCR products for G3PDH (**a**, *left*), *β*-tubulin (**a**, *right*), *β*-tubulin (**b**), or *arom* mRNA (**c**)

DHS and SK domains, respectively. A universally conserved glycine in the motif LGNAGTA of the EPSP domain was also found. This glycine is thought to be involved in the interaction with the substrate phosphoenolpyruvate (Padgette et al. 1991). We have also detected another EPSP synthase signature motif (DHR) of which the histidine residue was demonstrated to be at or near the active site of EPSP synthase (Huynh 1987).

We have reported that the relative substrate abundance of the in vitro SK assay (as compared to substrate concentrations occuring in vivo) might have prevented observation of the starvation effect, that is, detection of significant increases in AROM activity in cultures induced by 5.2 mM of quinate but growing in the absence of quinate as a carbon source (Liu et al. 2003a). In this study, results from two different experimental approaches, northern blot hybridization analysis (Fig. 6b) and suppression subtractive hybridization (Fig. 7c), showed that transcription of the *arom* gene did increase upon quinate induction in the virulent $M_2^-$ isolates Rhs 1AP and the hypovirulent $M_2^+$ Rhs 1A1. Assuming that increased *arom* transcription leads to elevated AROM activity, the data of this study suggests that the compensation or starvation phenomenon (as it applies to the *arom* gene) occurs in the basidiomycete *R. solani* as has been reported in the ascomycete *A. nidulans* Lamb et al. (1992).

The grouping of fungal taxa shown in Fig. 5 is based on the sequence of the full-length AROM protein. There was a clear separation between basidiomycetes and ascomycetes, and this is in agreement with widely accepted fungal systematics schemes (Alexopoulos et al. 1996) as well as the phylogeny of yeasts based on entire genome sequences (Dujon et al. 2004). In contrast, Campbell et al. (2004) attempted to resolve the phylogenetic relationships of eukaryotes including fungi using amino acid sequences of individual enzyme domains of the AROM protein and failed to differentiate between ascomycetes and basidiomycetes. They assumed that individual genes corresponding to these domains in fungi evolved inde-

pendently and therefore followed separate evolutionary histories, which was an invalid assumption due to two reasons. First, the order of five enzyme domains is the same on all of the fungal AROM sequences known to date, and second, in certain bacterial species, the shikimate pathway genes are clustered and co-transcribed as an operon (Parish and Stoker 2002; Ward et al. 2002). So, it is reasonable to assume that the entire shikimate pathway gene cluster was transferred to a eukaryotic ancestor. We further argue that phylogenetic relationships inferred by including full-length AROM protein sequences have a greater resolving power and could provide reliable genetic relationships among genera as shown in our study. Although more sequence data will be required to determine as to whether or not such a transfer from prokaryotes to eukaryotes (fungi) occurred more than once, our hypothesis is more parsimonious than the alternative of "multiple sequential fusion events coupled with rearrangements in domain order" resulting in a functional AROM protein as proposed by Campbell et al. (2004).

## References


Alexopoulos CJ, Mims CW, Blackwell M (1996) Introductory mycology, 4th edn. John Wiley, New York, 869 p

Bandy BP, Tavantzis SM (1990) Effect of hypovirulent *Rhizoctonia solani* on Rhizoctonia disease, growth, and development of potato. Am Potato J 67:189–199

Banerji SA, Wakefield E, Allen AG, Maskell DJ, Peters SE, Hopkin JM (1993) The cloning and characterization of the *arom* gene of *Pneumocystis carini*. J Gen Microbiol 139:2901–2914

Boosalis MG (1950) Studies on the parasitism of *Rhizoctonia solani* Kühn on soybeans. Phytopathology 40:820–831

Campbell SA, Richards TA, Mui EJ, Samuel BU, Coggins JR, McLeod R, Roberts CW (2004) A complete shikimate pathway in *Toxoplasma gondii*: an ancient eukaryotic innovation. Int J Parasitol 34(1):5–13

Carling DE (1996) Grouping in *Rhizoctonia solani* by hyphal anastomosis interactions. In: Sneh B, Jabaji-Hare S, Neate S, Dijst G (eds) *Rhizoctonia* species: taxonomy, molecular biology, ecology, pathology and disease control. Kluwer, Dordrecht, pp 37–47

Chamberlain VK, Wain RL (1971) Studies on plant growth-regulating substances-the influence of ring substituents on the plant growth regulating activity of phenylacetic acid. Ann Appl Biol 69:65–72

Charles IG, Keyte JW, Brammar WJ, Smith M, Hawkins AR (1986) The isolation and nucleotide sequence of the complex AROM locus of *Aspergillus nidulans*. Nucl Acids Res 14:2201–2213

Coggins JR, Boocock MR, Chaudhuri S, Lambert JM, Lumsden J, Nimmo GA, Smith DDS (1987a) The *arom* multifunctional enzyme from *Neurospora crassa*. Method Enzymol 142:325–341

Coggins JR, Duncan K, Anton IA, Boocock MR, Chaudhuri S, Lambert JM, Lewendon A, Millar G, Mousdale DM, Smith DDS (1987b) The anatomy of a multifunctional enzyme. Biochem Soc Trans 15:754–759

Davis RH, deSerres FJ (1970) Genetic and Microbiological Research Techniques for *Neurospora crassa*. Methods in Enzymology 17(a):79–143

Davis RH (1975) Compartmentalization and regulation of fungal metabolism: genetic approaches. Annual Review of Genetics 9:39–65

Diatchenko L, Lau YF, Campbell AP, Chenchik A, Moqadam F, Huang B, Lukyanov S, Lukyanov K, Gurskaya N, Sverdlov E.D, Siebert PD (1996) Suppression subtractive hybridization: a method for generating differentially regulated or tissue-specific cDNA probes and libraries. Proc Natl Acad Sci USA 93:6025–6030

Dujon B et al (2004) Genome evolution in yeasts. Nature 430:35–44

Duncan K, Edwards RM, Coggins JR (1987) The pentafunctional *arom* enzyme of *Saccharomyces cerevisiae* is a mosaic of monofunctional domains. Biochem J 246:375–386

Elliston JE (1982) Hypovirulence. Adv Plant Pathol 1:1–33

Frank JA, Francis SK (1976) The effect of a *Rhizoctonia solani* phytotoxin on potatoes. Can J Bot 54:2536–2540

Giles NH, Partridge CWH, Ahmed SE, Case ME (1967) The occurrence of the dehydroquinases in *Neurospora crassa*, one constitutive and one inducible. Proc Natl Acad Sci USA 58:1930–1937

Giles NH, Geever RF, Asch DK, Avalos J, Case ME (1991) Organizaton and regulation of the *qa* (quinic acid) genes in *Neurospora crassa* and other fungi. J Hered 82:1–7

Guo Z, Sherman F (1996) 3′-end-forming signals of yeast mRNA. Trends Biochem Sci 21:477–481

Hall TA (1999) BioEdit: a user-friendly biological sequence alignment editor and analysis program for Windows 95/98/NT. Nucl Acids Symp Ser 41:95–98

Hawkins AR, Giles NH, Kinghorn JR (1982) Genetical and biochemical aspects of quinate breakdown in the filamentous fungus *Aspergillus nidulans*. Biochem Genet 20:271–286

Hawkins AR, Lamb HK, Moore JD, Charles IG, Roberts CF (1993) The prechorismate (shikimate) and quinate pathways in filamentous fungi: theoretical and practical aspects. J Gen Microbiol 139:2891–2899

Hickok NJ, Seppanen PJ, Kontula KK, Janne PA, Bardin CW (1986) Two ornithine decarboxylase mRNA species in mouse kidney arise from size heterogeneity at their 3′ termini. Proc Natl Acad Sci USA 83:594–598

Huynh QK (1987) Reaction of 5-enolpyruvilshikimate-3-phosphate synthase with diethyl pyrocarbonate: evidence for an essential histidine residue. Arch Biochem Biophys 258:233–239

Jian J, Lakshman DK, Tavantzis SM (1997) Association of distinct double-stranded RNAs with enhanced or diminished virulence in *Rhizoctonia solani* infecting potato. Mol Plant Microbe Inter 10:1002–1009

Jianqiang M, Chirala SS, Wakil SJ (2003) Human acetyl-CoA carboxylase 1 gene: presence of three promoters and heterogeneity at the 5′-untranslated mRNA region. Proc Natl Acad Sci USA 100:7515–7520

Kozak M (1987) An analysis of 5′-noncoding sequences from 699 vertebrate messenger RNAs. Nucl Acids Res 15:8125–8148

Kumar S, Tamura K, Jakobsen IB, Nei M (2001) MEGA2: molecular evolutionary genetics analysis software. Bioinformatics 12:1244–1245

Lakshman DK, Jian J, Tavantzis SM (1998) A novel mitochondrial double-stranded RNA found in a hypovirulent strain of *Rhizoctonia solani* occurs in DNA form, and is phylogenetically related to the pentafunctional AROM protein of the shikimate pathway. Proc Natl Acad Sci USA 95:6425–6429

Lamb HK, van der Hombergh JPTW, Newton GH, Moore JD, Roberts CF, Hawkins AR (1992) Differential flux through the quinate and shikimate pathways: implications for the channeling hypothesis. Biochem J 284:181–187

Lamb HK, Newton GH, Levett LJ, Cairns E, Roberts CF, Hawkins AR (1996) The QUTA activator and QUTR repressor proteins of *Aspergillus nidulans* interact to regulate transcription of the quinate utilization pathway genes. Microbiology 142:1477–1490

Liu C, Lakshman DK, Tavantzis SM (2003a) Quinic acid induces hypovirulence, and expression of a hypovirulence-associated double-stranded RNA in *Rhizoctonia solani*. Curr Genet 43:103–111

Liu C, Lakshman DK, Tavantzis SM (2003b) Expression of a hypovirulence-causing double-stranded RNA (dsRNA) is associated with up-regulation of quinic acid pathway, and down-regulation of shikimic acid pathway in *Rhizoctonia solani*. Curr Genet 42:284–291

Logemann J, Schell J, Willmitzer L (1987) Improved method for the isolation of RNA from plant tissues. Anal Biochem 163:16–20

Marchler-Bauer A, Bryant SH (2004) CD-Search: protein domain annotations on the fly. Nucl Acids Res 32:W327–W331

Milborrow BV, Purse JG, Wightman F (1975) On the auxin activity of phenylacetic acid. Ann Bot 39:1143–1146

Padgette SR, Biest RED, Gasser CS, Eichholtz DA, Frazier RB, Hironaka CM, Levine EB, Shah DM, Fraley RT, Kishore GM (1991) Site-directed mutagenesis of a conserved region of the 5-enolpruvylshikimate-3-phosphate synthase active site. J Biol Chem 266:22364–22369

Pain A, Woodward J, Quail MA, Anderson MJ, Clark R, Collins M, Fosker N, Fraser A, Harris D, Larke N, Murphy L, Humphray S, O'Neil S, Pertea M, Price C, Rabbinowitsch E, Rajandream MA, Salzberg S, Saunders D, Seeger K, Sharp S, Warren T, Denning DW, Barrell B, Hall N (2004) Insight into the genome of *Aspergillus fumigatus*: analysis of a 922 kb region encompassing the nitrate assimilation gene cluster. Fungal Genet Biol 41(4):443–453

Parish T, Stoker NG (2002) The common aromatic amino acid biosynthesis pathway is essential in *Mycobacterium tuberculosis*. Microbiology 148:3069–3077

Pauws E, van Kampen1 AHC, van de Graaf SAR, de Vijlder JJM, Ris-Stalpers C (2001) Heterogeneity in polyadenylation cleavage sites in mammalian mRNA sequences: implications for SAGE analysis. Nucl Acids Res 29:1690–1694

Rossman MG, Moras D, Olsen KW (1974) Chemical and biological evolution of a nucleotide binding protein. Nature 250:194–199

Saitou N, Nei M (1987) The neighbor joining method: a new method for reconstructing phylogenetic trees. Mol Biol Evol 4:406–425

Sambrook J, Fritsch EF, Maniatis T (1989) Molecular cloning. A laboratory manual, 2nd edn. Cold Spring Harbor, New York

Sherwood RT, Lindberg CG (1962) Production of a phytotoxin by *Rhizoctonia solani*. Phytopathology 52:586–587

Shyamala V, Ferro-Luzzi Ames G (1993) Single specific primer-polymerase chain reaction (SSP-PCR) and genome walking. In: Bruce A (eds) PCR protocols current methods and applications, Chap 32, White. Humana Press, New Jersey, pp 339–348

Sneh B, Jabaji-Hare S, Neate S, Dijst G (eds) (1996) *Rhizoctonia* species: taxonomy, molecular biology, ecology, pathology and disease control. Kluwer, Dordrecht, 578 p

Strauss EE, Lakshman DK, Tavantzis SM (2000) Molecular characterization of the genome of a partitivirus from the basidiomycete *Rhizoctonia solani*. J Gen Virol 81:549–555

Tavantzis SM (ed) (2001) DsRNA genetic elements: concepts and applications in agriculture, forestry and medicine. CRC Press LLC, Boca Raton, 304 p

Tavantzis SM, Lakshman DK (1995) Virus-like double-stranded RNA elements and hypovirulence in phytopathogenic fungi, Chap 17. In: Kohmoto K, Singh RP, Singh US (eds) Pathogenesis and host-parasite specificity in plant disease: histopathological, biochemical, genetic and molecular basis, vol III. Elsevier (Pergamon) Press, Oxford, pp 249–267

Tavantzis SM, Perkins BL, Bushway RJ, Bandy BP (1989) Correlation between in vitro synthesis of phenylacetic acid and virulence in *Rhizoctonia solani*. Phytopathology 79:1199

Walker JE, Saraste M, Runswick MJ, Gay NJ (1982) Distantly related sequence in the $\alpha$ and $\beta$ subunits of ATP synthase, myosin. Kinases, and other ATP- requiring enzymes and a common nucleotide binding fold. EMBO J 1:945–951

Ward DE, De Vos WM, Van Der Oost J (2002) Molecular analysis of the role of two aromatic aminotransferases and a broad-specificity aspartate aminotransferase in the aromatic amino acid metabolism of *Pyrococcus furiosus*. Archaea 1:133–141

Wood V et al (2002) The genome sequence of Schizosaccharomyces pombe. Nature 415:871–880

Wyllie TD (1962) Effect of metabolic by-products of *Rhizoctonia solani* on the roots of Chippewa soybean seedlings. Phytopathology 52:202–206